Automated Motion Artifacts Removal between Cardiac Long- and Short-axis Magnetic Resonance Images

Maria C Carminati[1], Francesco Maffessanti[2], Enrico G Caiani[1]

[1] Biomedical Engineering Department, Politecnico di Milano, Milano, Italy
[2] Centro Cardiologico Monzino, IRCSS, Milano, Italy

Abstract

We aimed at developing and testing an automated method for motion artifacts compensation, to reduce potential misalignment between short-axis (SAX) and two- and four-chamber long-axis (2ch4chLAX) cardiac magnetic resonance (CMR) images that could introduce artifacts in advanced 3D volumetric analysis, thus precluding accurate measurements.

Each SAX slice of the CMR dataset is shifted by optimizing normalized cross correlation of pixel intensities at slice intersection with 2ch4chLAX. The algorithm accuracy has been tested in a dedicated phantom study and applied to a clinical dataset consisting of end diastolic (ED) and end systolic (ES) CMR SAX and 2ch4chLAX frames obtained in 10 consecutive patients.

The algorithm performance evaluated on the phantom dataset provided the residual displacement error after images correction (range values 0 - 2.5 mm), with registration errors comparable with the pixel resolution. Application to clinical data, comparing by visual inspection the results with and without correction, resulted in a perceived improvement in 52.9% *of the analyzed frames, thus proving feasibility and usefulness of the method as a necessary pre-processing step for volumetric analysis of CMR data in clinical setting.*

1. Introduction

Cardiac magnetic resonance (CMR) imaging represents the gold standard for ventricular volumes and mass quantification. To this aim, the common acquisition protocol is based on the acquisition of dynamic images in the short-axis view (SAX) from base to apex, from which endocardial and epicardial contours are semi-automatically detected and utilized for cavity volume and mass computation by the method of disks [1]. However, the low coronal resolution of of SAX images (up to 10 mm slice thickness) makes the apex and the valvular plane definition subjected to uncertainties, and the incorrect inclusion of a slice can introduce a bias in the measurements. The volumetric analysis could be achieved with improved accuracy by combining SAX images with those acquired in the long-axis (LAX) view. In this way the SAX low resolution along their orthogonal direction by generating a 3D volumetric dataset allowing for advanced contour detection methods adoption [2–4].

Before recombining SAX and LAX views, a pre-processing step appears mandatory to correct possible mis-registration artifacts, which are mainly due to respiration. In fact, as each of the SAX and LAX dynamic image sequences is performed during different patient's apnea, breath-hold misalignment could occur due to the non exact repeatability of this maneuver over all acquisitions, thus generating relative shift in slices from different image series [2]. These artifacts are more prone to happen in heart failure patients, where the ability to maintain breathold is highly compromised. Moreover, breathing activity could also cause few degrees rotations of the heart that can be considered as minor artifact, and therefore neglected in first instance [5].

Based on these observations, our aims were: 1) to develop an automated method for compensating potential movement artifacts between different slices in SAX images, on the basis of their intersections with the LAX data; 2) to validate its performance by dedicated virtual phantom datasets featuring known relative movements, and by comparison with visual "gold standard" to evaluate the improvement in SAX-LAX registration when applied to clinical CMR datasets.

2. Methods

2.1. Phantom datasets

Two different volumetric virtual phantom 3D datasets were created. The first phantom consisted of a white cylinder on a black background (100x100x100 voxels, with 1x1x1 mm spacing). From this 3D data, three different datasets were extracted using the direction cosines relevant to three real CMR patient datasets. Each dataset, ob-

tained by linear interpolation, was constituted by four cut-planes, simulating a single SAX projection, and a LAX two chamber (2ch), four chamber (4ch) and three chamber (3ch) views.

The second phantom was obtained from a patient cardiac computed tomographic (CT) 3D frame (GE Medical System, 512x512x399 voxels with spacing 0.51x0.51x0.4 mm): a dataset of three cut-planes was obtained by trilinear interpolation, simulating a single SAX projection and LAX 2ch and 4ch slices, computed from the planes orientation of the CMR data of the same patient.

First, the CT frame and CMR data were rigidly registered (6 degrees of freedom, dof) using a multiresolution inter-modal voxel-based approach, driven by normalized mutual information cost function and gradient descent optimizer [6]. The registration framework was developed using the open source ITK library [7]. To ensure temporal correspondence, both SAX MR and 3D CT frame were chosen at 40% of cardiac cycle. Then, the retrieved coordinates transformation was applied to SAX and 2ch4chLAX direction cosines to obtain plane orientations for SAX and LAX plane extraction on the CT frames:

$$\begin{aligned} T_{SAX-CT} &= T_{SAX} \times T_{MR}^{CT} \\ T_{LAX-CT} &= T_{LAX} \times T_{MR}^{CT} \end{aligned} \quad (1)$$

where T_{MR}^{CT} is the 4x4 transformation matrix resulting from the rigid registration, T_{SAX} and T_{LAX} include original direction cosines and image position patient of SAX and LAX images, T_{LAX-CT} and T_{SAX-CT} represent the final cutting planes used to recreate LAX and SAX slices from CT data.

2.2. Slice displacement simulation

In this study, the simulation of the displacement due to respiration artifacts on the phantom datasets was focused on in-plane translation of the SAX image (i.e. two degrees of freedom), as the movement due to the heart beating is handled by ECG gating [5]. The displacements were defined as translations in x- and y- directions of the SAX image plane with respect to the upper left corner of the image (origin of the coordinate system), corresponding to the image position patient of SAX CMR data. Therefore, z-axis is coincident to the left ventricular long-axis, resulting in a patient-specific reference system. Range of values of the imposed displacements were chosen between (-7: +7) pixels in each direction, corresponding to a (-3.57: +3.57) mm in the CT dataset.

2.3. Artifacts correction

The proposed method for motion artifacts compensation is based on the maximization of the normalized cross correlation (NCC) of pixel intensities along the intersections between SAX and LAX planes. The resulting correction is a 3D translation along the plane of the direction cosines, resulting in a 2 dof transformation. As a first step, pixel value profiles at the intersections between the SAX and the LAX images have been computed. The metric that guides the correction is the NCC computed between the profiles on the SAX image and the corresponding ones on each LAX image, according to:

$$NCC(d) = \frac{\sum_i [(x_i - m_x)\,(y_{i-d} - m_y)]}{\sqrt{\sum_i (x_i - m_x)^2}\,\sqrt{\sum_i (y_{i-d} - m_y)^2}} \quad (2)$$

where x_i and y_i are the two series of pixel values to be correlated, m_x and m_y are their corresponding mean values, and d is the distance between series. The search domain for the optimal position of the SAX image was defined as a neighborhood of ± 10 pixels around the original position of the SAX plane defined by the image position patient and decomposed in the x- and y- directions (Figure 1). Starting from the original position, the SAX image was shifted within the search domain and, at each step, profile values at SAX-LAX intersections and cross correlation values were computed. Finally, the optimal correction was defined as the displacement in the admissible spatial domain featuring maximum mean cross correlation values at each intersection, and applied to the SAX image. The method was developed using the VTK open source visualization toolkit [8].

2.4. Error estimate

The algorithm performance has been evaluated analyzing the residual error as a result of algorithm phantom datasets with known displacement:

$$err = \frac{\sum_{i=1}^{N} \sqrt{(\delta x_i - \delta x_i')^2 + (\delta y_i - \delta y_i')^2}}{N} \quad (3)$$

where δx_i and δy_i are the known displacements applied to the SAX image, $\delta x_i'$ and $\delta y_i'$ are the computed corrections along the x and y axes of the SAX plane for the i^{th} simulated displacement, and N is the number of simulated movements.

2.5. Clinical MR data evaluation

To test the algorithm performance on real clinical data, retrospectively selected dynamic, ECG-gated, steady-state free precession images acquired in SAX and 2ch4chLAX during breath hold (GE Healthcare, 1.5T) in 10÷20 slices from the atrium to the apex in 10 consecutive patients (20 or 30 phases/cardiac cycle, pixel spacing 0.7422 or 1.5652 mm, slice thickness 8 mm with no overlap and no gap), were selected.

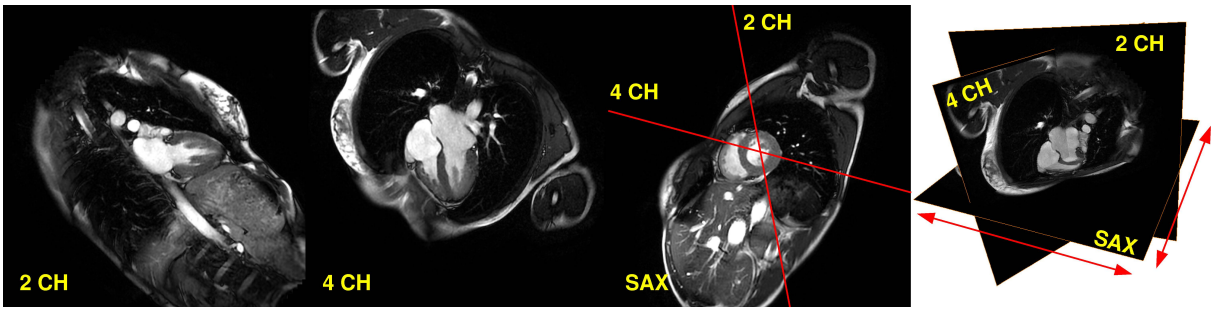

Figure 1. 4D cine MR sequence in 2ch long-axis, 4ch long-axis views, a midventricular short-axis 2D view and in 3D coordinate system

The end-diastolic (ED) and end-systolic (ES) frames were utilized for the following analysis: an experienced cardiologist was asked to visualize the 3D data corresponding to the intersecting 2ch4chLAX with each of the SAX planes, with the original data (without motion correction) randomly visualized on one half of the screen and the corrected data on the other half. Navigation of the dataset was automatically applied on both half-screens, to guarantee the same orientation and scale. The cardiologist was asked for each SAX plane to evaluate which, if any, of the two visualized datasets was the most aligned in terms of left atrial and ventricular endocardial contours matching. The algorithm performance was then evaluated by counting the number of SAX planes in which the chosen half-screen corresponded to the corrected or to the original dataset and in terms of range of the applied shifts. Images were excluded if image planes were below the apex or if characterized by other evident artifacts.

3. Results

The results of the proposed method applied to the first phantom (cylinder datasets) are presented in Table 1. Two different types of projections of the SAX image were considered: axial and non-axial. In the first case, the SAX plane corresponded to the axial projection of the cylinder, i.e. the SAX image was representing a circle, while in the second case the SAX plane did not correspond to the axial projection of the cylinder, resulting in an oblique projection of the object.

The influence of the number of LAX images used as reference on the overall performance has been assessed considering 2 (2ch and 4ch) or 3 (2ch, 4ch and 3ch) LAX images, to investigate the potential increase of information contribution achieved by including also the 3ch image. As showed, the use of the third plane did not reduce the potential errors in the alignment, probably due to the interpolation process.

The test on the second phantom, based on a real CT dataset, was performed by setting the step size equal to one pixel (0.51 mm) and using only two LAX views (2ch and 4ch). A SAX view was extracted and misaligned as described in section 2.2, and subsequently corrected. In this case, the mean error computed according to Eq.3 was equal to 0.06 mm. The computation time of the algorithm correction was approximately 1.5 s on a general purpose laptop.

Table 1. Correction errors [mm] for the three datasets created from the cylinder volumetric image. SAX plane is defined either as axial and non axial projection of the cylinder.

Subject	2ch4chLAX [mm]		2ch3ch4chLAX [mm]	
	axial	non-axial	axial	non-axial
1	0.12	0.95	0.17	0.95
2	0.16	0.17	0.16	0.17
3	0.97	2.05	0.95	1.93

In the evaluation of the algorithm performance in the clinical data, a total number of 242 slices was visually compared, with and without correction. The corrected images were judged better than the original in 128/242 slices (52.9%) (Figure 2), worst in 16/242 slices (6.6%) and with no visual difference in 98/242 slices (40.5%). Interestingly, in 67/98 of the datasets perceived as equivalent (68.3% corresponding to the 27.7% of all cases) a minimal correction, arbitrarily defined as an absolute displacement of maximum 2 pixels per direction, was present and thus correctly defined as non different datasets.

The analysis of the range of the applied shifts by the correction resulted in $0 - 18.2$ mm (median value and interquartile difference equal to 3.1 mm and 3.7 mm, respectively), with the ED range $0 - 18.2$ mm (3.1 mm and 3.9 mm) slightly larger than the ES range $0 - 16.8$ mm (3.3 mm and 3.9 mm).

Mean computational time per SAX slice was 0.7 s, with a mean value of 0.9 s for the 5 patients with 0.7422 mm pixel spacing and 0.5 s for the remaining 5 patients with 1.5652 mm pixel spacing, due to the size of the algorithm

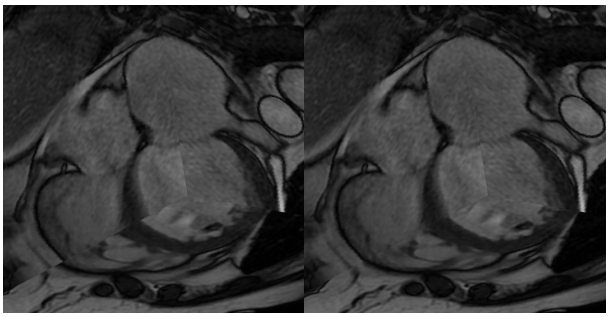

Figure 2. CMR before (left) and after (right) correction

step, defined as 1 pixel.

4. Discussion

We presented a novel method that proposes the use of LAX images for CMR SAX movement artifacts correction. The algorithm was tested on virtual phantoms, resulting in errors comparable with the pixel resolution. In the binary phantom better results were found when the SAX image was extracted as the axial projection of the cylinder, while larger errors characterized non-axial projections, probably due to the effect of the linear interpolation step in the correction process. In both cases, the performance varied depending on the orientations planes from which the virtual images were created, proving reliance with the linear approximation used to create the data. The potential use of additional LAX data (i.e. 3ch view) to increase the information contribution was also investigated in the binary phantom, but without showing clear improvements that justify its utilization (with increase in algorithm complexity and computational time).

The CT-derived phantom, representing real cardiac anatomical data, reported a reduced residual error, indicating that the method is dependent on the information content of the input image. Also, the results confirmed that 2ch and 4ch LAX only were able to drive correctly the algorithm to convergence.

The evaluation of the performance on real clinical data showed a noticeable improvement in data, thus justifying its application as a necessary pre-processing step when data analysis has not to be based just on disk-summation method, in particular when a volumetric surface detection analysis has to be applied to directly compute LV volumes or to be utilized for advanced finite element model analysis [9].

5. Conclusions

The results of the phantom validation confirm the method functionality and envisage its clinical applicability. Future work will be focused on the extension of the displacement simulation adding a degree of freedom, i.e. the translation on the z-axis of the SAX plane, by adding one dimension to the search domain. This would provide more accurate results, allowing to simulate the effect of the base-to-apex LV motion during systole.

Furthermore, even if phantom analysis suggested that 2ch and 4ch LAX views alone are able to drive the correction algorithm, the additional use of the 3ch LAX view or multiplanar LAX views could contribute to an even improved the correction of the clinical data.

References

[1] Petitjean C, Dacher J. A review of segmentation methods in short axis cardiac MR images. Med Image Anal 2011; 15(2):169–184.

[2] Lötjönen J, Järvinen V, Cheong B, Wu E, Kivistö S, Koikkalainen J, Mattila J, Kervinen H, Muthupillai R, Sheehan F, et al. Evaluation of cardiac biventricular segmentation from multiaxis MRI data: a multicenter study. JMRI J Magn Reson Im 2008;28(3):626–636.

[3] Rahman S, Wesarg S. Combining short-axis and long-axis cardiac MR images by applying a super-resolution reconstruction algorithm. SPIE Medical Imaging 2010 Image Processing 2010;11.

[4] Saring D, Relan J, Groth M, Mullerleile K, Handels H. 3D segmentation of the left ventricle combining long-and short-axis MR images. Method Inform Med 2010;48(4):340.

[5] McLeish K, Hill D, Atkinson D, Blackall J, Razavi R. A study of the motion and deformation of the heart due to respiration. IEEE T Med Imaging 2002;21(9):1142–1150.

[6] Carminati M, Maffessanti F, Gripari P, Pontone G, Andreini D, Pepi M, Caiani E. A framework for CT and MR image fusion in cardiac resynchronization therapy. In Computing in Cardiology, volume 39. 2012; in press.

[7] Ibanez L, Schroeder W, Ng L, Cates J. The ITK Software Guide. Kitware, Inc. ISBN 1-930934-10-6, http://www.itk.org/ItkSoftwareGuide.pdf, first edition, 2003.

[8] Schroeder W, Martin K, Lorensen B. The Visualization Toolkit: An object oriented approach to 3d graphics. new york: Kitware. Inc Publisher 2003;.

[9] Conti C, Votta E, Corsi C, De Marchi D, Tarroni G, Stevanella M, Lombardi M, Parodi O, Caiani E, Redaelli A. Left ventricular modelling: a quantitative functional assessment tool based on cardiac magnetic resonance imaging. Interface Focus 2011;1(3):384–395.

Address for correspondence:

Maria Chiara Carminati
Politecnico di Milano, Biomedical Engineering Dpt,
Piazza L. da Vinci, 32, 20133 Milan, Italy
maria.carminati@mail.polimi.it